Calcium-Induced Structural Transition in the Regulatory Domain of Human Cardiac Troponin C[†,‡]

Leo Spyracopoulos,[§,||] Monica X. Li,[§,||] Samuel K. Sia,[§] Stéphane M. Gagné,[§] Murali Chandra,[⊥] R. John Solaro,[⊥] and Brian D. Sykes*[,§]

MRC Group in Protein Structure and Function, Department of Biochemistry, University of Alberta, Edmonton, Alberta T6G 2H7, Canada, and Department of Physiology and Biophysics, University of Illinois at Chicago, Chicago, Illinois 60612

Received May 23, 1997; Revised Manuscript Received July 30, 1997[⊗]

ABSTRACT: While calcium binding to troponin C (TnC) triggers the contraction of both skeletal and cardiac muscle, there is clear evidence that different mechanisms may be involved. For example, activation of heart myofilaments occurs with binding to a single regulatory site on TnC, whereas activation of fast skeletal myofilaments occurs with binding to two regulatory sites. The physiological difference between activation of cardiac and skeletal myofilaments is not understood at the molecular level due to a lack of structural details for the response of cardiac TnC to calcium. We determined the solution structures of the apo and calcium-saturated regulatory domain of human cardiac TnC by using multinuclear, multidimensional nuclear magnetic resonance spectroscopy. The structure of apo human cardiac TnC is very similar to that of apo turkey skeletal TnC even though there are critical amino acid substitutions in site I. In contrast to the case with the skeletal protein, the calcium-induced conformational transition in the cardiac regulatory domain does not involve an "opening" of the regulatory domain, and the concomitant exposure of a substantial hydrophobic surface area. This result has important implications with regard to potential unique aspects of the interaction of cardiac TnC with cardiac troponin I and of modification of cardiac myofilament regulation by calcium-sensitizer drugs.

The troponin complex is a critical unit of muscle thin filament that regulates muscle contraction through the binding of Ca^{2+} to troponin C (TnC)[1] [for reviews, see Farah and Reinach (1995), Grabarek et al. (1992), Leavis and Gergely (1984), Tobacman (1996) and Zot and Potter (1987)]. Calcium binding initiates a cascade of structural changes in the thin filament complex that lead to muscle contraction. It is believed that the conformational change of TnC upon Ca^{2+} binding releases the inhibition of actin−myosin reaction by TnI and activates muscle contraction. There are two isoforms of TnC whose expression is dependent upon tissue type and regulation during development. sTnC is a component of mammalian fast skeletal muscle, whereas cTnC is a constituent of slow skeletal and cardiac muscle. A large body of structural data has allowed for a detailed understanding of the molecular basis of Ca^{2+} regulation in sTnC, but there is a complete lack of structural details for the analogous mechanism in the cardiac isoform.

The X-ray structures of avian sTnC show a highly α-helical protein with two domains of about 80 amino acids joined by a central helix, each domain being composed of two Ca^{2+}-coordinating E-F hand moieties (Herzberg & James, 1988; Satyshur et al., 1988). The two Ca^{2+} binding sites in the N terminus of TnC (I and II) are regulatory sites (Potter & Gergely, 1975; Putkey et al., 1989, 1991; Szczensna et al., 1996) and have a lower affinity for Ca^{2+} relative to those in the C domain (III and IV), which are believed to assume a structural role (Negele et al., 1992). The Herzberg−Moult−James model for the conformational change of the regulatory N domain of sTnC upon Ca^{2+} binding was proposed on the basis of a comparison between the apo N domain and the Ca^{2+}-saturated C domain (Herzberg et al., 1986). The exact details of the Ca^{2+}-induced conformational change were recently elucidated with the description of the apo and Ca^{2+}-saturated NMR solution structures of the N domain of sTnC (Gagné et al., 1995) and the NMR solution structure of Ca^{2+}-saturated intact sTnC (Slupsky & Sykes, 1995). The solution structures of the sNTnC revealed that the conformational response to Ca^{2+} in sTnC involves an "opening" of the structure and the concomitant exposure of a substantial hydrophobic surface area. It is believed that exposure of the hydrophobic patch alters the interaction between sTnI and sTnC, and subsequently, the interaction of TnI with F-actin is disrupted. Ultimately, F-actin interacts with the myosin head, and the power stroke slides the thin filament past the myosin complex to achieve muscle contraction.

The primary structures of the skeletal and cardiac TnC proteins display a high degree of similarity. However, in the case of cTnC, mutation of critical side chain ligands (D29L and D31A) and an insertion (Val-28) (van Eerd &

[†] Supported by the MRC Group in Protein Structure and Function, the Heart and Stroke Foundation of Canada, and the National Institutes of Health (Grant HL 49934).

[‡] The atomic coordinates for the final structures and the sets of restraints have been deposited with the Brookhaven Protein Data Bank (accession codes 1SPY and 1AP4).

* To whom correspondence should be addressed. E-mail: brian.sykes@ualberta.ca.

[§] University of Alberta.

[||] Both Authors contributed equally to this work.

[⊥] University of Illinois at Chicago.

[⊗] Abstract published in *Advance ACS Abstracts,* September 15, 1997.

[1] Abbreviations: N- or CTnC, N- or C-terminal domain of troponin C, respectively; s- or cTnC, skeletal or cardiac-troponin C, respectively; s- or cTnI, skeletal or cardiac troponin I, respectively; HSQC, heteronuclear single-quantum coherence; NMR, nuclear magnetic resonance; NOE, nuclear Overhauser effect; rmsd, root mean square deviation.

S0006-2960(97)01223-3 CCC: $14.00

Takahashi, 1975) have abolished the ability of site I to coordinate Ca^{2+}. Thus, site II is primarily responsible for regulation of contraction in cardiac and slow muscle (Putkey et al., 1989, 1991). For sNTnC, the opening of the hydrophobic pocket requires the stepwise binding of two Ca^{2+} ions to functionally coupled sites I and II (Li et al., 1995). A recent structural study of an sTnC mutant with an altered site I (E41A-sNTnC) revealed a closed conformation in the Ca^{2+}-saturated state and provided evidence that the critical step for the opening of sNTnC is Ca^{2+} binding to site I (Gagné et al., 1997). On the basis of the structure of Ca^{2+}−E41A-sNTnC, it was suggested that the regulatory domain of cTnC which also contains a defunct site I will be in a closed conformation in the Ca^{2+}-saturated state (Gagné et al., 1997). This proposal contradicts present expectations. Specifically, models of the molecular mechanism of Ca^{2+} regulation for cTnC proposed to date suggest that the regulatory domain adopts an open conformation in response to Ca^{2+}, much like the skeletal isoform (Pollesello et al., 1994; Rao et al., 1995). The impetus for suggesting an open conformation for cTnC is derived from the fact that Ca^{2+} binding to TnC is the trigger for contraction in muscle. The effect of the trigger event must be transferred to other components of the thin filament assembly for contraction to occur. Therefore, it is not surprising that the key regulatory step in the contraction of cardiac muscle is generally assumed to be accompanied by a large change in the structure and energetics of the regulatory protein, as observed for sNTnC (Gagné et al., 1995).

The NMR structure of mutant intact chicken Ca^{2+}-saturated cTnC (C35S and C84S) has been solved recently (Sia et al., 1997), but details of the transition from the apo to the Ca^{2+}-saturated state remain unknown. In the present study, we have determined the solution structures of the regulatory N domain of apo and Ca^{2+}-saturated wild type human cTnC using multinuclear, multidimensional NMR spectroscopy. The validity of studying the isolated N domain is based on the observation that the measured Ca^{2+} binding constant for site II in the N domain is the same as that measured for intact cTnC (Li et al., 1997). Additionally, it is known that the Ca^{2+} binding properties of the skeletal N domain remain unchanged when it is separated from intact sTnC (Li et al., 1994, 1995). Surprisingly, the structures show that cNTnC remains closed upon binding Ca^{2+}. These results have profound implications for the interaction of cTnC with TnI and the regulation of contraction in cardiac muscle.

MATERIALS AND METHODS

Sample Preparation. The engineering of the expression vector of cNTnC (1−89) was as described in Chandra et al. (1997). The expression of ^{15}N- and $^{15}N/^{13}C$-labeled protein in *Escherichia coli* was as described previously for sNTnC (Gagné et al., 1994; Li et al., 1995). Purification of the protein was achieved as previously described for cleaved sTnC (Golosinska et al., 1991). Calcium-free cNTnC was obtained in a manner similar to that of Ca^{2+}-free sNTnC (Li et al., 1995). NMR samples contained 500 μL of either 9:1 H_2O/D_2O or 99.996% D_2O (pH 6.7), 100 mM KCl, 15 mM fresh DTT, and 1.5−3.0 mM protein. Calcium-saturated samples of cNTnC contained 6−8 mM Ca^{2+}. Samples of Ca^{2+}-free cNTnC contained 15 mM EDTA.

NMR Spectroscopy. All the NMR spectra were obtained using Unity INOVA 500 MHz or Unity 600 MHz spectrometers equipped with triple-resonance probe heads and *z*-axis pulsed field gradients. All NMR spectra were acquired at 30 °C. Spectra processing and analysis were accomplished with the programs NMRPipe (Delaglio et al., 1995) and PIPP (Garrett et al., 1991), respectively. Sequential assignment of the backbone resonances was achieved using three-dimensional (3D) $^1H-^{15}N$ Noesy HSQC (150 ms) (Zhang et al., 1994) and CBCA(CO)NNH (Grzesiek & Bax, 1992; Muhandiram & Kay, 1994) experiments in H_2O at 600 MHz for the apoprotein and a combination of the 3D HNCACB (Wittekind & Mueller, 1993; Muhandiram & Kay, 1994) and CBCA(CO)NNH experiments in H_2O at 600 MHz for the Ca^{2+}-loaded protein. Side chain resonance assignments were accomplished with the HCCH-TOCSY experiment in H_2O at 500 MHz (Bax et al., 1990; Kay et al., 1993).

Structure Determination. Interproton distance restraints were obtained from ^{15}N-separated 3D NOESY HSQC (Zhang et al., 1994) and simultaneous $^{15}N/^{13}C$-separated 3D NOESY HSQC (75 ms) in H_2O (Pascal et al., 1994). Distance restraints for the 75 ms 3D NOESY experiments were calibrated as previously described (Gagné et al., 1997), with the error on the peak intensities set to 40%, and the lower bound on all proton−proton restraints set to 1.7 Å. On the basis of homologous calcium binding sites, six distance restraints of 2.0−2.8 Å to the Ca^{2+} ion in site II were assigned (Strynadka & James, 1989). The ϕ angle dihedral restraints were obtained from $^3J_{HNH\alpha}$ coupling constants derived from 3D HNHA spectra acquired in H_2O at 500 MHz (Vuister & Bax, 1993). For the HNHA experiment, a correction factor of 1.055 was used, peak intensities were assumed to have errors of 25%, and the minimum restraint range was set to ±20°. The $d_{N\alpha}/d_{\alpha N}$ ratio was used to obtain loose dihedral restraints for the ψ angle of -30 ± 110 or $110 \pm 110°$, as reported previously (Gagné et al., 1994). All valine and leucine methyl groups for Ca^{2+}−cNTnC as well as three of seven valines and five of six leucines for apo-cNTnC were stereospecifically assigned using a ^{13}C HSQC of a 30% ^{13}C-labeled sample (Neri et al., 1989). The side chain Hβ-methylene protons were stereospecifically assigned using $^3J_{H\alpha H\beta}$ and $^3J_{HNH\beta}$ values from the experiments with 3D HACAHB spectra in D_2O at 500 MHz (Grzesiek et al., 1995) and 3D HNHB in H_2O at 500 MHz (Archer et al., 1991), respectively. Restraints for the χ_1 angle of 60, 180, or −60° (±60°) were imposed if the $^3J_{H\alpha H\beta}$ and $^3J_{HNH\beta}$ coupling constants were consistent with only one side chain rotamer.

The initial sets of restraints for apo- and Ca^{2+}−cNTnC contained no dihedral restraints, and a fraction of the NOEs given in Table 1. These initial sets of restraints were used to calculate 100 starting structures starting from an extended conformation using the simulated annealing protocol in XPLOR with 60 ps of heating and 30 ps of cooling for the apoprotein and 50 ps of heating and 30 ps of cooling for the Ca^{2+}-saturated protein. Approximately 50% of the initial structures converged. Structure refinement was carried out starting with 43 (apo) and 45 (Ca^{2+}) converged structures using the XPLOR simulated annealing protocol with 30 ps of heating and 20 ps of cooling for the apoprotein and 50 ps of heating and 30 ps of cooling for Ca^{2+}−cNTnC. For the Ca^{2+}−cNTnC, the Ca^{2+} restraints were added in the later stages of refinement. The final ensemble consisted of 40 structures with the lowest total energy in the family of refined structures.

Table 1: Characteristics of the Solution Structures of Apo- and Ca^{2+}−cNTnC

	apo-cNTnC	Ca^{2+}-cNTnC
distance restraints		
total	1213	1344
intraresidue	494	561
sequential ($\|i-j\|=1$)	297	307
medium ($2 \le \|i-j\| \le 4$)	255	305
long ($\|i-j\| \ge 5$)	167	171
dihedral restraints	48 ϕ, 23 ψ, 11 χ_1	53 ϕ, 21 ψ, 23 χ_1
restraints violation		
distance of >0.2 Å	7 (0.18/structure)	0
dihedral of >2°	0	0
rmsd (Å)[a]		
well-defined regions[b]		
backbone atoms	0.61 ± 0.11	0.61 ± 0.09
heavy atoms	1.10 ± 0.09	1.02 ± 0.07
helix[c]	0.28	0.25
site I (residues 28−40)	0.69 ± 0.29	0.53 ± 0.18
site II (residues 63−71)	0.82 ± 0.19	0.38 ± 0.09
ϕ/ψ in the most-favored region (all residues)[d] (%)	81.1%	81.5%

[a] Forty structures for apo- and Ca^{2+}−cNTnC were calculated using the simulated annealing (Nilges et al., 1988) protocol within XPLOR 3.1 (Brünger, 1992). [b] Well-defined regions were residues 5−27, 34−65, and 70−84 for apo-cNTnC and residues 5−84 for Ca^{2+}−cNTnC. [c] The average of the N and A−D backbone rmsds when each helix is separately superimposed to its average. [d] Backbone dihedral angle distributions were determined with the program PROCHECK (Laskowski et al., 1993).

RESULTS

NMR Spectra. Figure 1 shows the high-quality {^{1}H-^{15}N}-2D-HSQC spectra obtained for both apo- and Ca^{2+}−cNTnC. The backbone amide resonances are completely assigned for apo- and Ca^{2+}-saturated cNTnC with the exception of M1 and D2 which were not observed due to rapid exchange with solvent. The backbone amide resonances display line widths characteristic of a protein of ∼10 kDa at 30 °C for the apo and Ca^{2+}-saturated states of cNTnC. The Ca^{2+}-saturated spectrum shows some additional line broadening for resonances in sites I and II. Calcium titrations of ^{15}N-labeled cNTnC, monitored by following chemical shift changes in {^{1}H−^{15}N}2D-HSQC NMR spectra, confirmed that Ca^{2+} binds to only one site in cNTnC (Li et al., 1997). Spectra of cNTnC are not hampered by line broadening caused by Ca^{2+}-induced dimerization, as observed for the skeletal isoform (Gagné et al., 1994, 1995; Slupsky et al., 1995a). For example, triple-resonance 3D NMR spectra used to obtain the backbone through bond sequential connectivities are also of high quality (Figure S1 in the Supporting Information).

Description of the Structures. The secondary structural characteristics of apo- and Ca^{2+}−cNTnC are similar. There are five helices, a nonfunctional Ca^{2+} binding site, and a functional Ca^{2+} binding site, which are joined by a twisted antiparallel β-sheet, as defined in Figure 2. Helices B and C are joined by a six-residue linker (Figure 2A,B). The binding of Ca^{2+} to site II in cNTnC results in a slight reorientation of the B and C helices (see Figure 2A,B and Table 3). The N, A, and D helices form a structural unit (NAD unit), which remains invariant to Ca^{2+} binding, superimposing with an rmsd of 0.74 Å for apo- and Ca^{2+}−cNTnC. The high quality of the solution structures is indicated in Tables 1 and 2. There are no NOE violations greater than 0.2 Å in the family of 40 NMR structures for both apo- and Ca^{2+}−cNTnC, except for residues 28 and 29 at the beginning of site I of the apoprotein, which were found to be undergoing conformational exchange *via* ^{15}N-relaxation measurements (unpublished data). The α-helices are well-defined, superimposing with individual rmsds of 0.20 ± 0.06 (N), 0.38 ± 0.09 (A), 0.21 ± 0.07 (B), 0.33 ± 0.10 (C), and 0.26 ± 0.06 Å (D) for apo-cNTnC and 0.23 ± 0.06 (N), 0.29 ± 0.08 (A), 0.23 ± 0.06 (B), 0.27 ± 0.07 (C), and 0.23 ± 0.06 Å (D) for Ca^{2+}−cNTnC (Figure 2A,B). The antiparallel β-sheet is well-defined with an rmsd of 0.14 ± 0.04 (apo) and 0.21 ± 0.05 Å (Ca^{2+}). The N- and C-terminal residues (residues 1−4 and 86−89) as well as the linker region (49−53) are less well-defined than the helices and β-sheet. The functional and defunct Ca^{2+}-binding sites are less well-defined than the helices for both the apo and Ca^{2+}-loaded structures. Sites I and II are more well-defined in the Ca^{2+}-saturated state with an rmsd of about 0.4 Å for Ca^{2+}−cNTnC compared to 0.7 Å for apo-cNTnC (Table 1). The interhelical orientations for the apo structure are somewhat less well-defined than the individual helices, and the overall structure superimposes with an rmsd of 0.76 Å, compared to 0.61 Å for the Ca^{2+}-loaded structure (using residues 5−84 for apo- and Ca^{2+}-cNTnC). The program PROCHECK (Laskowski et al., 1993) was used to determine the distribution of backbone dihedral angles. For all residues,

Table 2: Statistics of the Conformational Energies and rmsd for the Ensemble of Structures for cNTnC

	apo-cNTnC	Ca^{2+}−cNTnC
energy (kcal mol^{-1})		
total	97 ± 3	95 ± 2
bonds	1.6 ± 0.2	1.5 ± 0.1
angles	79 ± 1	78 ± 7
impropers	12.0 ± 0.1	12.2 ± 0.2
van der waals (F_{repel})[a]	2 ± 1	2 ± 1
NOE restraints[b]	2.0 ± 1.4	1.5 ± 0.4
dihedral restraints[b]	0.02 ± 0.02	0.02 ± 0.02
rmsd from experimental restraints		
NOE distance restraints (Å)	0.006 ± 0.002	0.005 ± 0.001
dihedral angle restraints (deg)	0.05 ± 0.03	0.04 ± 0.03
rmsd from ideal covalent geometry		
bonds (Å)	0.00107 ± 0.00005	0.00105 ± 0.00004
angles (deg)	0.457 ± 0.004	0.450 ± 0.002
impropers	0.340 ± 0.002	0.340 ± 0.002

[a] The force constant for the van der Waals energy (F_{repel}) calculation was 4.0 kcal mol^{-1} Å^{-4}. [b] Force constants for calculation of NOE and dihedral energies were 50 and 200 kcal mol^{-1}, respectively.

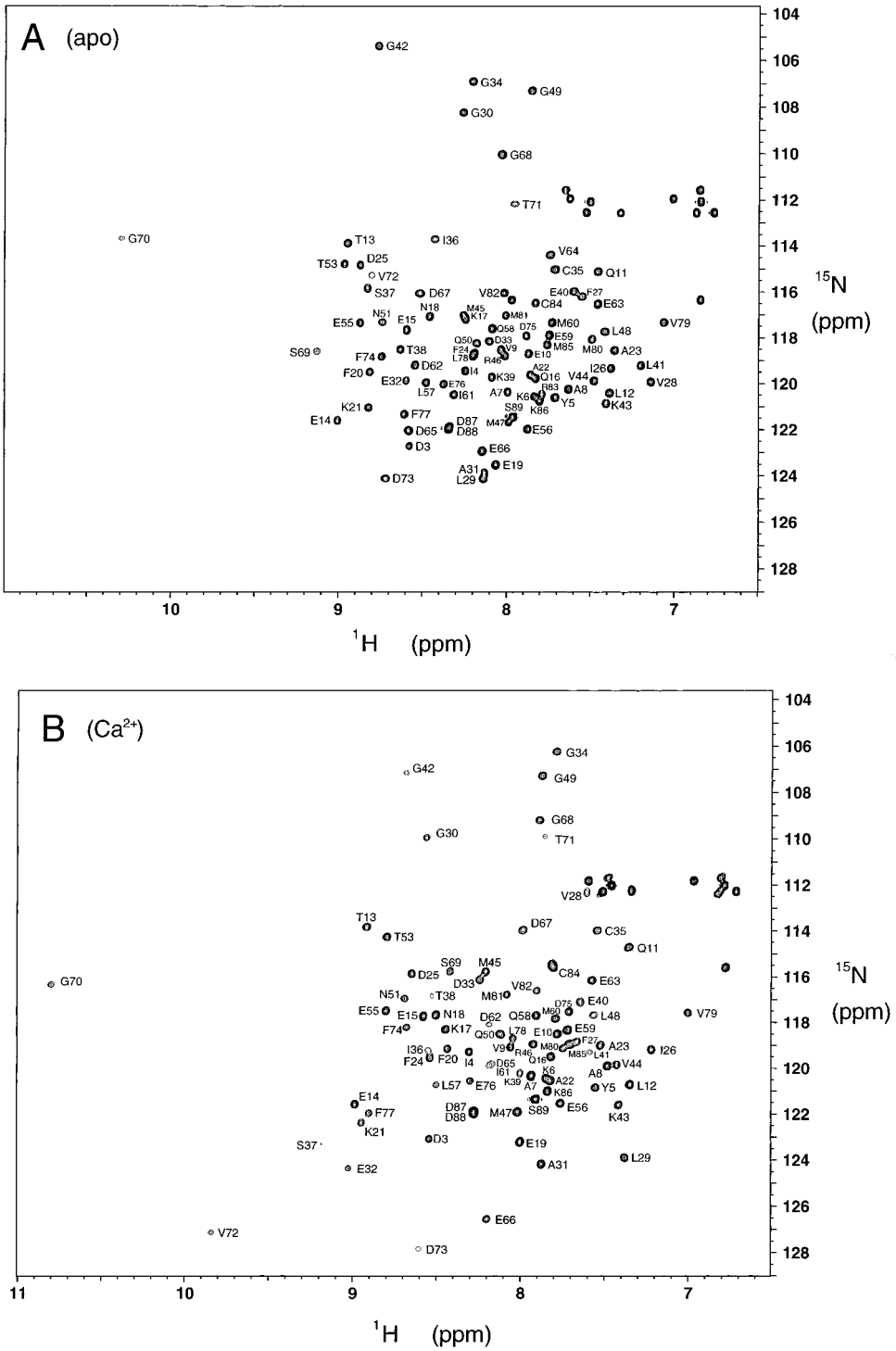

FIGURE 1: Amide regions of the {$^{1}H-^{15}N$}-HSQC NMR spectra of 1.6 mM (A) apo-cNTnC (without EDTA) and (B) cNTnC with 4.5 equiv of Ca^{2+}. Other sample conditions are as described in Materials and Methods. Spectra were obtained with 512 complex points in t_2 and 64 complex points in t_1 at 500 MHz with WALTZ-16 decoupling (Shaka et al., 1983) during acquisition. The spectral widths were 7000 and 1500 Hz in t_2 and t_1, respectively.

81% (apo) and 82% (Ca^{2+}) of the ϕ and ψ angles fell into the most-favored regions, and a further 16% (apo) and 17% (Ca^{2+}) were distributed within the additional allowed region.

The interhelical angle between the C and D helices changes by 12° upon binding of Ca^{2+} (Table 3). A comparison of backbone dihedral angles between apo-sNTnC, $2Ca^{2+}-$sNTnC, and $2Ca^{2+}-$E41A-sNTnC reveals that the "hinge" about which the end of the C helix rotates relative to the NAD unit occurs at Val-65 (Val-64 in cTnC) (Gagné et al., 1997). The coupling constant for Val-64 determined from the 3D HNHA experiment for apo-cNTnC is 8.4 Hz, close to the expected value of 7.4 Hz for a closed conformation of Val-65 in sNTnC (Gagné et al., 1997). Although this coupling constant was not measurable from the 3D HNHA experiment for $Ca^{2+}-$cNTnC due to exchange broadening, the backbone ϕ angles at this residue for the family of structures are $-92 \pm 12°$ for apo-cNTnC and $-98 \pm 15°$ for $Ca^{2+}-$cNTnC, indicating that there is only a small change in the orientation of the C helix upon Ca^{2+} binding.

The B helix reorients very slightly relative to the A helix when Ca^{2+} binds site II in cNTnC (Table 3). The B helix hinge in site I, which is analogous to the C helix hinge (Val-

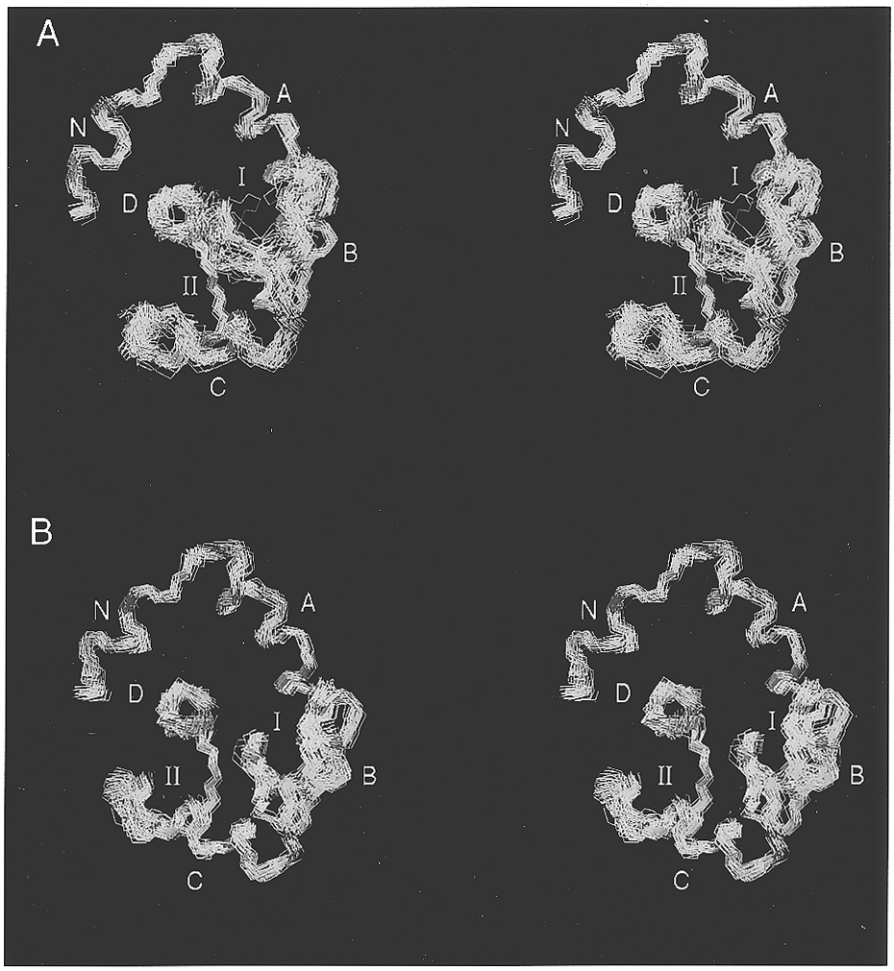

FIGURE 2: Structure of the regulatory domain of cNTnC in apo and Ca^{2+}-saturated states. (A) Backbone superposition of the 40 structures of apo-cNTnC (residues 5−84). The α-helices N (5−11), A (14−26), B (38−48), C (54−64), and D (74−84) and the twisted β-sheet (35−37 and 71−73) are well-defined. The linker (49−53) and sites I and II (28−40 and 65−76, respectively) are less well-defined than the helices. (B) Backbone superposition of the 40 strucutures of Ca^{2+}−cNTnC. The secondary structure is similar to apo-cNTnC with helices N (5−11), A (14−27), B (41−48) C (54−62), and D (74−84) and β-sheet (35−37 and 71−73), and sites I and II, although less well-defined than the helices, are better defined than the sites in apo-cNTnC.

Table 3: Interhelical Angles for cNTnC and sNTnC

	A/B	B/C	C/D	A/D
apo-cNTnC	136 ± 3	118 ± 4	129 ± 5	113 ± 3
Ca^{2+}−cNTnC	132 ± 3	106 ± 4	117 ± 3	116 ± 3
apo N domain of sTnC (X-ray)[a]	134	128	147	116
apo-sNTnC (NMR)[b]	130 ± 3	126 ± 5	125 ± 4	111 ± 2
sNTnC−2Ca^{2+} (NMR)[c]	90 ± 3	100 ± 6	69 ± 5	109 ± 3

[a] PDB accession code 5TNC. [b] PDB accession code 1TNP. [c] PDB accession code 1TNQ.

64), is Glu-40 in cNTnC. There is ample evidence that Glu-41 in sNTnC is the hinge involved in the straightening of the B helix on Ca^{2+} binding to sNTnC (Gagné et al., 1994, 1995, 1997). The $^3J_{HNH\alpha}$ determined for Glu-40 from the 3D HNHA experiment is 8.7 Hz for apo-cNTnC and 7.7 Hz for Ca^{2+}−cNTnC, corresponding to ϕ dihedral restraints of −101 ± 20 (apo) and −88 ± 20° (Ca^{2+}), indicating that Ca^{2+} binding causes a small change at the hinge of the B helix. For the ensemble of solution structures, the ϕ dihedral angle of Glu-40 in the apo state (−91 ± 9°) indicates a kink at the N terminus of the B helix, which persists upon binding Ca^{2+} (−99 ± 7°).

The Ca^{2+}-induced structural change of cNTnC involves small reorientations of the B and C helices relative to the NAD unit. Furthermore, the total exposed nonpolar accessible surface area using the Shrake definitions (Shrake & Rupley, 1973) for residues 5−84 is 2701 ± 82 Å^2 for the apo state and 2719 ± 63 Å^2 when Ca^{2+} binds to site II in cNTnC. The major hydrophobic pocket of cNTnC in the apo and Ca^{2+}-saturated states occurs at the interface of the A−D helices and involves residues Phe-20, Ala-23, and Phe-24 of the A helix, Leu-41, Val-44, and Met-45 of the B helix, Leu-57, Ile-61, and Val-64 of the C helix, and Val-72, Val-77, Leu-78, Met-80, and Met-81 of the D helix. The main hydrophobic pocket exposes 96 Å^2 in the apo state compared to 132 Å^2 in the Ca^{2+}-saturated state. There are also hydrophobic contacts between the N and D helices involving residues Tyr-5, Ala-8, Val-9, Leu-78, Val-79, Val-82, and Arg-83.

DISCUSSION

The structural data presented here show for the first time the Ca^{2+}-induced structural transition in the regulatory domain of cardiac troponin C. The BC structural unit in cNTnC moves only slightly away from the NAD structural unit in cNTnC. This movement is only a fraction of the analogous change in the skeletal isoform. The global fold of apo-cNTnC is very similar to that of apo-sNTnC, apart from a slightly different orientation of the N helix within

the NAD structural unit. The interhelical angles of apo-cNTnC are comparable to those of apo-sNTnC, indicative of a closed conformation for the apo state of the regulatory domain in both isoforms. The structure of Ca^{2+}−cNTnC differs significantly from that of Ca^{2+}−sNTnC, displaying interhelical angles and a total exposed hydrophobic surface area that are expected for a closed conformation. The structures of apo- and Ca^{2+}−cNTnC presented herein are a crucial advance in understanding the basis of myocardial contraction. Furthermore, diseases such as myocardial infarction are thought to involve a desensitization of myocardium to Ca^{2+}, resulting in a failure of the myocardium to contract in response to the Ca^{2+} trigger (Lee & Allen, 1990). Knowledge of the 3D solution structure of cardiac TnC is clearly important in answering various clinically relevant questions such as the design of pharmacological agents for improving cardiac performance and the development of rational therapies for heart failure.

Comparison to Intact cTnC. The Ca^{2+}-saturated structure of human cNTnC is similar to the structure of the N domain of Ca^{2+}-saturated intact mutant (C35S/C84S) chicken cTnC reported recently (Sia et al., 1997). The backbone atoms of the NAD unit of the N domain of intact chicken cTnC superimpose with rmsds of 1.13 and 0.97 Å with the apo and Ca^{2+}-saturated N domain of human cNTnC, respectively. The total exposed hydrophobic surface area of the N domain of intact chicken cTnC is 3030 ± 68 Å^2 for residues 2−87 (Sia et al., 1997), similar to those of the apo- and Ca^{2+}-saturated cNTnC, which are 3090 ± 86 and 3108 ± 71 Å^2, respectively. The interhelical angles for the intact Ca^{2+}−cTnC are similar to those for the Ca^{2+}−cNTnC, indicating that both Ca^{2+}−cNTnC and Ca^{2+}−cTnC remain in a predominantly closed conformation upon Ca^{2+} binding. This is evidence showing that separation of the two domains has little structural effect on the regulatory domain, as corroborated by Ca^{2+} binding studies of the isolated domain (Li et al., 1997). Mutation of the cysteine residues in the regulatory domain appears to have little effect on the structure of the regulatory domain.

Comparison to Structural Change in Skeletal NTnC. The secondary structure of apo- and Ca^{2+}−cNTnC is similar to that found in the apo- and Ca^{2+}−sNTnC solution structures (Gagné et al., 1994) and the N domain of the intact sTnC solution structure (Slupsky et al., 1995b). The N and A−D helices and the antiparallel β-sheet span similar lengths over analogous residues in the cardiac protein. Interestingly, the kink in the B helix at Glu-40 in apo-cNTnC (Glu-41 is the analogous residue in sNTnC) remains upon Ca^{2+} binding to cNTnC. The backbone dihedral angles at this residue are known to change to α-helical values as sNTnC undergoes a gross conformational change involving straightening of the B helix upon Ca^{2+} binding (Gagné et al., 1994, 1995). The ϕ dihedral angle at Glu-40 and the interhelical angles of the B helix (Table 3) in the apo and Ca^{2+} states indicate that the B helix in the cardiac protein does not straighten to the same extent as sNTnC upon Ca^{2+} binding.

The solution structure of Ca^{2+}-free cNTnC is similar to the solution structure (Gagné et al., 1995) and the crystal structure (Herzberg & James, 1988; Satyshur et al., 1988) of apo-sNTnC. The values of the interhelical angles (Table 3) indicate that the helices of apo-cNTnC are packed similarly with respect to the skeletal isoform. The rmsd for the backbone atoms upon superimposing apo-sNTnC with apo-cNTnC is 1.20 Å and Ca^{2+}−cNTnC with Ca^{2+}−sNTnC is 1.57 Å; both values are larger than the rmsds for the NAD superposition of apo-cNTnC with Ca^{2+}−cNTnC (0.74 Å) and apo-sNTnC with Ca^{2+}−sNTnC (0.80 Å), and these differences are due primarily to the orientation of the N helix in the two isoforms of the protein (using residues 5−27 and 74−84 in cNTnC and analogous residues 7−29 and 75−85 in sNTnC). The angle between the N and A helix in sNTnC is 116 (apo) and 120° (Ca^{2+}), compared to 107 (apo) and 99° (Ca^{2+}) for the cardiac protein. However, this structural difference is likely a reflection of the nonspecific role of the N helix (Liu et al., 1994) rather than a reflection of any unique functional properties generated in the adoption by the N helix of a new interhelical angle. Additionally, the N helix was found to be more flexible than the A and D helices of the NAD structural unit, as determined by ^{15}N-relaxation measurements (unpublished data).

Although the NAD structural unit of Ca^{2+}-saturated cNTnC is similar to the NAD unit in sNTnC, the orientation of the BC unit relative to the NAD unit is different in the two isoforms of the protein. The Ca^{2+}-saturated cardiac regulatory domain displays interhelical angles similar to those in the apo state (closed conformation), whereas the skeletal protein shows changes in the interhelical angles between the NAD and BC structural units of up to 56° (Table 3).

The difference in total exposed hydrophobic surface area between the apo- and Ca^{2+}-saturated protein can be used to compare the extent of opening between the two isoforms of NTnC. The cardiac isoform of the N domain changes from 3090 ± 86 Å^2 for apo-cNTnC to 3108 ± 71 Å^2 for Ca^{2+}−cNTnC (residues 2−87), while in sNTnC, the total exposed hydrophobic surface area changes from 2866 to 3386 Å^2 (equivalent residues 4−88) upon binding of Ca^{2+}, an increase of 502 Å^2 compared to that of cNTnC (Figure 3). In fact, residues in the hydrophobic core of apo-sNTnC which experience an increase in exposed hydrophobic surface area greater than 19−20 Å^2 upon Ca^{2+} binding (Ala-25, Val-45, Met-46, Ile-61, Met-81, and Met-82) (Strynadka et al., 1997) are found to undergo only small changes in exposed surface area when Ca^{2+} binds the N domain of the cardiac isoform (Ala-23, Val-44, Met-45, Met-60, Met-80, and Met-81).

Comparison to E41A-sNTnC. E41A-sNTnC and cNTnC have substitutions within site I (compared to sTnC) that abolish the ability of Glu-40 (Glu-41 in sNTnC) to coordinate Ca^{2+}. The structure of 2Ca^{2+}−E41A-sNTnC reveals that Ca^{2+} binding to site II in E41A-sNTnC does not result in an opening of the structure to the same extent as that of native sNTnC. The C/D interhelical angle in 2Ca^{2+}−E41A-sNTnC is only 5° greater than that of the apo form of sNTnC (Gagné et al., 1997). In addition, the ϕ dihedral angle at Ala-41 is close to that for Glu-41 in apo-sNTnC, indicative of a closed conformation for Ca^{2+}−E41A-sNTnC. The central conclusion of the E41A-sNTnC structural study is that binding of Ca^{2+} to site I and coordination to the bidentate ligand side chain of Glu-41 in particular are the essential mechanisms underlying the opening of sNTnC. Although E41A-sNTnC and cNTnC possess different mutations in the site I E-F hand ligands, both proteins are unable to coordinate Ca^{2+} at the sixth residue (−*Z* position) of the E-F hand helix−loop−helix motif. The −*Z* position occurs at the beginning of the B helix in sNTnC (E41) and cNTnC (E40). The straightening of the B helix upon Ca^{2+} coordination to the bidentate ligand side chain of Glu-41 (sNTnC) or Glu-40 (cNTnC) is

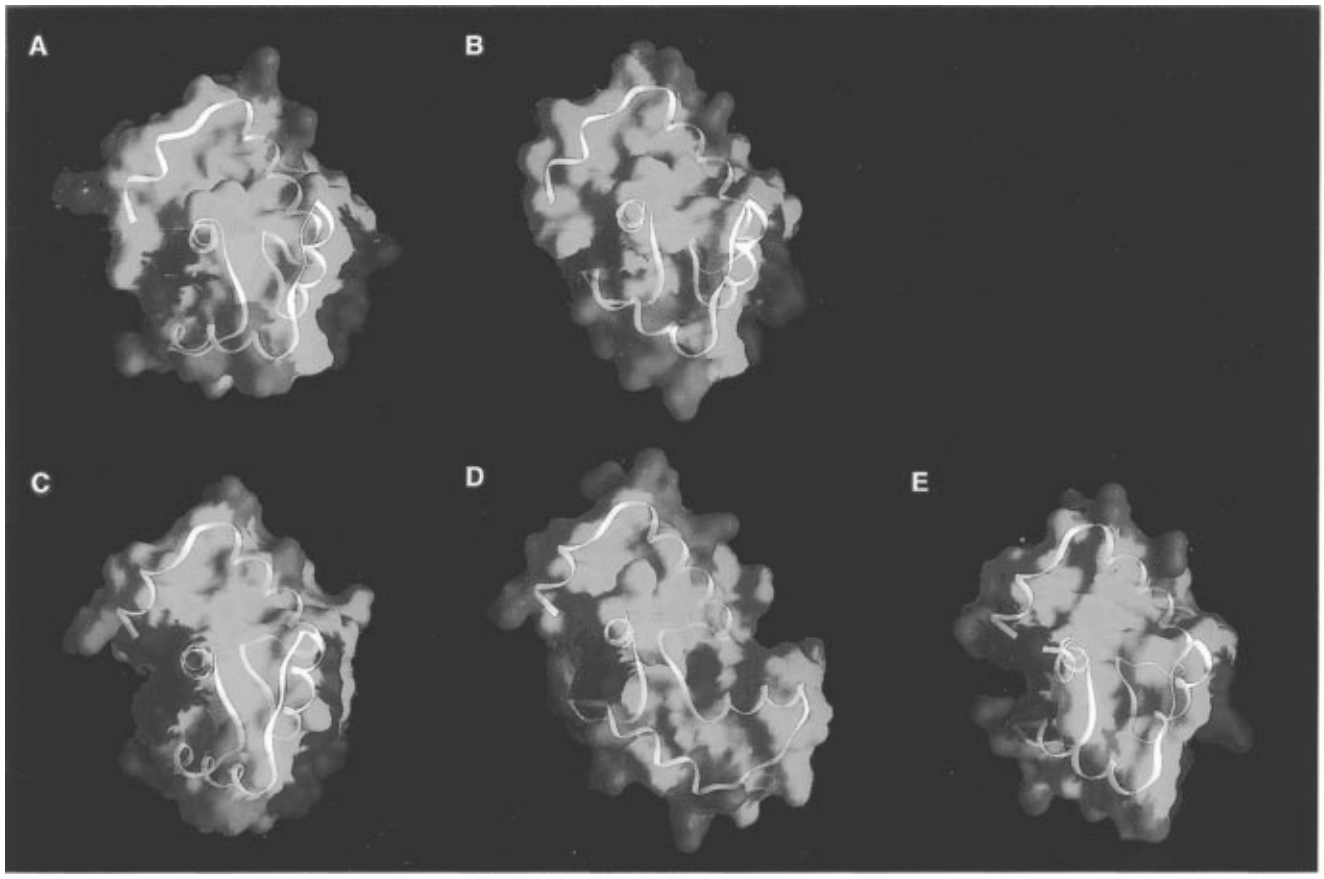

FIGURE 3: Comparison of the molecular surfaces of (A) apo-cNTnC and (B) Ca^{2+}−cNTnC (residues 5−84), (C) apo-sNTnC and (D) Ca^{2+}−sNTnC, and (E) E41A-sNTnC (residues 7−85). The backbone atoms of residues 5−27 and 74−84 of the cardiac isoform were superimposed onto the backbone residues (7−29 and 75−85) of the skeletal protein. The structures are oriented as in Figure 2. Positively charged residues (Arg and Lys) are shown in blue. Negatively charged residues (Asp and Glu) are shown in red. Hydrophobic residues (Ala, Ile, Leu, Met, Phe, Pro, Tyr, and Val) are shown in yellow. Polar residues are shown in white (Asn, Gln, Gly, Ser, and Thr). The program GRASP was used to create the figure (Nicholls, 1992).

believed to be a crucial step in the opening of TnC (Gagné et al., 1997; Sia et al., 1997). E41A-sNTnC lacks the $-Z$ ligand entirely, and cTnC cannot coordinate any Ca^{2+} in site I due to the absence of the *X* and *Y* ligands. Thus, both cNTnC and E41A-sNTnC cannot undergo a Ca^{2+}-dependent opening due to the inability of the $-Z$ ligand in site I to coordinate Ca^{2+}. Taken together, these results provide a clear understanding of the Ca^{2+}-induced structural transition in sNTnC and also mimic the Ca^{2+}-induced conformational transition in cNTnC.

Relevance to the paired E-F Hand Mechanism. Despite the inability of site I to bind Ca^{2+}, it is evident from $^3J_{HNH\alpha}$ coupling constants and backbone ^{15}N-relaxation measurements (unpublished data) that sites I and II are structurally coupled in cNTnC. Interestingly, site II shows $^3J_{HNH\alpha}$ coupling constants which are not averaged to random coil values in both the apo and Ca^{2+}-saturated states, whereas the coupling constants in site I show random coil values in the apo state but not in the Ca^{2+}-bound state. These results suggest that site II is predisposed to Ca^{2+} binding. Binding of Ca^{2+} to site II leads to a decrease in the flexibility of the backbone residues in site I, an entropic loss which is compensated for by ligation of Ca^{2+} to the carboxylate ligands in site II. This observation provides insight into the mechanism of Ca^{2+} binding in the coupled E-F hands in sNTnC. The initial binding of Ca^{2+} to site II prepares site I for Ca^{2+} binding and, ultimately, for the critical ligation of the bidentate carboxylate ligand Glu-41 to Ca^{2+}, as recently suggested (Gagné et al., 1997; Li et al., 1995). This suggestion is also corroborated by a detailed comparison of the structure of apo-sNTnC and the recently determined structure of Ca^{2+}−sNTnC, as determined by X-ray crystallography, which indicates that site II is predisposed to Ca^{2+} binding (Strynadka et al., 1997).

There are two classes of Ca^{2+} binding proteins that share the paired E-F hand motif (Chazin, 1995). Regulatory proteins such as calmodulin and troponin C bind target peptides and proteins and undergo large interhelical movements upon Ca^{2+} binding (Finn et al., 1995; Gagné et al., 1995; Kuboniwa et al., 1995; Zhang et al., 1995), and buffering proteins such as calbindin D_{9K} (Skelton et al., 1995), which do not undergo large scale conformational changes upon Ca^{2+} binding. The Ca^{2+}-bound state of cNTnC presented herein sets a precedent for regulatory E-F hand proteins. The interhelical reorientations of cNTnC upon Ca^{2+} binding are closer to those expected for buffering proteins. On the other hand, troponin C in cardiac muscle operates in tandem with other proteins within a ternary complex, and it is not clear whether cTnC binds its target protein (cTnI) in an open conformation in intact muscle.

Relevance with Respect to Function. It is surprising that such a small conformational change accompanies Ca^{2+} binding to cNTnC, given that the N domain is the principal regulatory protein of contraction in cardiac muscle, and that the skeletal isoform displays one of the largest known Ca^{2+}-induced conformational changes in E-F hand proteins.

However, a closed conformation for the regulatory domain is consistent with the following observations. First, the mutant $2Ca^{2+}$−E41A-sNTnC is unable to properly coordinate Ca^{2+} at the $-Z$ ligand in site I and remains closed when Ca^{2+} binds. Second, the affinity between sTnC and skeletal TnI in the presence of Ca^{2+} is 4-fold greater than the affinity of cTnC for TnI in the presence of Ca^{2+} (Liao et al., 1994). The mutations within site I serve to increase the barrier to cTnC−cTnI complex formation by removing electrostatic interactions between Ca^{2+} and site I carboxylate ligands, which balance the entropic loss associated with exposing the hydrophobic surface. Thus, the diminished affinity of cTnC for cTnI in the presence of Ca^{2+}, relative to the skeletal proteins, may be interpreted by a reduction in hydrophobic protein−protein interactions between cTnC and cTnI, a direct consequence of the closed conformation in Ca^{2+}−cNTnC. However, the possibility that the cardiac regulatory domain binds cTnI in an open conformation cannot be ruled out. For example, the ^{13}C and ^{1}H chemical shifts for the ϵ-methyl group of Met-81 in cTnC change dramatically in the presence of cTnI (Krudy et al., 1994), yet this residue is buried in both the apo and Ca^{2+}-saturated states (side chain accessible surface areas of 9 ± 9 and 8 ± 4 Å^2, respectively). On the other hand, Met-80 is also buried (apo, 1.7 Å^2; Ca^{2+}, 7.8 Å^2) and does not experience chemical shift changes on cTnI binding (Krudy et al., 1994), whereas the analogous residues in sNTnC (Met-81 and Met-82) experience an increase of 42 and 51 Å^2, respectively, in side chain accessible surface area upon binding of Ca^{2+} (Strynadka et al., 1997).

Relevance to the Design of Pharmacological Agents for Treatment of Heart Failure. A possible therapeutic treatment for heart failure involves the enhancement of the response of myofilaments to Ca^{2+} with little or no change in intracellular levels of Ca^{2+}. Cardiac TnC has been proposed as the target molecule for binding of drugs such as trifluoroperazine, bepridil, pimobendan, and levosimendan (Haikala et al., 1995; Pollesello et al., 1994). These drugs sensitize the myofilaments to Ca^{2+} and increase the Ca^{2+}-induced tension in muscle. Knowledge of the 3D solution structure of drug-bound cNTnC is crucial for the rational design of Ca^{2+}-sensitizer drugs, which enhance the Ca^{2+} affinity of the protein. Drug binding studies to date have been interpreted on the basis of the assumption that Ca^{2+}-saturated cTnC assumes an open conformation similar tothat for sTnC. Clearly, the design and binding studies of pharmaceuticals will benefit from the structures of cNTnC presented herein.

ACKNOWLEDGMENT

The assistance of D. Corson and L. Golden in the preparation of the cNTnC samples is gratefully acknowledged. We thank L. E. Kay for providing pulse sequences, G. McQuaid for maintenance of the NMR spectrometers, J. L. Willard, T. Jellard, and R. Boyko for computer expertise, and the Protein Engineering Network Centre of Excellence (PENCE) for the use of the Unity 600 NMR spectrometer.

SUPPORTING INFORMATION AVAILABLE

One figure (S1) showing $^{13}C_{\alpha/\beta}$ strips for the first twenty residues of apo- and Ca^{2+}−cNTnC taken from the 3D CBCA(CO)NNH spectra (2 pages). Ordering information is given on any current masthead page.

REFERENCES

Archer, S. J., Ikura, M. I., Torchia, D. A., & Bax, A. (1991) *J. Magn. Reson. 95*, 636−641.
Bax, A., Clore, G. M., & Gronenborn, A. M. (1990) *J. Magn. Reson. 88*, 425−431.
Brünger, A. T. (1992) *X-PLOR Version 3.1: A System for X-ray Crystallography and NMR*, Yale University Press, New Haven, CT.
Chandra, M., Dong, W.-J., Pan, B.-S., Cheung, H. C., & Solaro, R. J. (1997) *Biochemistry* (submitted for publication).
Chazin, W. J. (1995) *Nat. Struct. Biol. 2*, 707−710.
Delaglio, F., Grzesiek, S., Vuister, G. W., Zhu, G., Pfeifer, J., & Bax, A. (1995) *J. Biomol. NMR 6*, 277−293.
Farah, C. S., & Reinach, F. C. (1995) *FASEB J. 9*, 755−767.
Finn, B. E., Evenäs, J., Drakenberg, T., Waltho, J. P., Thulin, E., & Forsén, S. (1995) *Nat. Struct. Biol. 2*, 777−783.
Gagné, S. M., Tsuda, S., Li, M. X., Chandra, M., Smillie, L. B., & Sykes, B. D. (1994) *Protein Sci. 3*, 1961−1974.
Gagné, S. M., Tsuda, S., Li, M. X., Smillie, L. B., & Sykes, B. D. (1995) *Nat. Struct. Biol. 2*, 784−789.
Gagné, S. M., Li, M. X., & Sykes, B. D. (1997) *Biochemistry 36*, 4386−4392.
Garrett, D. S., Powers, R., Gronenborn, A. M., & Clore, G. M. (1991) *J. Magn. Reson. 95*, 214−220.
Golosinska, K., Pearlstone, J. R., Borgford, T., Oikawa, K., Kay, C. M., Carpenter, M. R., & Smillie, L. B. (1991) *J. Biol. Chem. 266*, 15797−15809.
Grabarek, Z., Tao, T., & Gergely, J. (1992) *J. Muscle Res. Cell Motil. 13*, 383−393.
Grzesiek, S., & Bax, A. (1992) *J. Am. Chem. Soc. 114*, 6291−6293.
Grzesiek, S., Kuboniwa, H., Hinck, A. P., & Bax, A. (1995) *J. Am. Chem. Soc. 117*, 5312−5315.
Haikala, H., Kaivola, J., Nissinen, E., Wall, P., Levijoki, J., & Lindén, I.-B. (1995) *J. Mol. Cell. Cardiol. 27*, 1859−1866.
Herzberg, O., & James, M. N. G. (1988) *J. Mol. Biol. 203*, 761−779.
Herzberg, O., Moult, J., & James, M. N. G. (1986) *J. Biol. Chem. 261*, 2638−2644.
Kay, L. E., Xu, G. Y., Singer, A. U., Muhandiram, D. R., & Forman-Kay, J. D. (1993) *J. Magn. Reson., Ser. Biol.*, 333−337.
Krudy, G. A., Kleerekoper, Q., Guo, X., Howarth, J. W., Solaro, R. J., & Rosevear, P. R. (1994) *J. Biol. Chem. 269*, 23731−23735.
Kuboniwa, H., Tjandra, N., Grzesiek, S., Ren, H., Klee, C. B., & Bax, A. (1995) *Nat. Struct. Biol. 2*, 768−776.
Laskowski, R. A., MacArthur, M. W., Moss, D. S., & Thorton, J. M. (1993) *J. Appl. Crystallogr. 26*, 283−290.
Leavis, P. C., & Gergely, J. (1984) *CRC Crit. Rev. Biochem. 16*, 235−305.
Lee, J. A., & Allen, D. G. (1990) *Br. Med. J. 300*, 551−552.
Li, M. X., Chandra, M., Pearlstone, J. R., Racher, K. I., Trigo-Gonzalez, G., Borgford, T., Kay, C. M., & Smillie, L. B. (1994) *Biochemistry 33*, 917−925.
Li, M. X., Gagné, S. M., Tsuda, S., Kay, C. M., Smillie, L. B., & Sykes, B. D. (1995) *Biochemistry 34*, 8330−8340.
Li, M. X., Gagné, S., Spyracopoulos, L., Kloks, C. P. A. M., Audette, G., Chandra, M., Solaro, R. J., Smillie, L. B., & Sykes, B. D. (1997) *Biochemistry* (submitted for publication).
Liao, R., Wang, C.-K., & Cheung, H. C. (1994) *Biochemistry 33*, 12729−12734.
Liu, W., Dotson, D. G., Lin, X., Mullen, J. J., III, Gonzalez-Garay, M. L., Lu, Q., & Putkey, J. A. (1994) *FEBS Lett. 347*, 152−156.
Muhandiram, D. R., & Kay, L. E. (1994) *J. Magn. Reson., Ser. B 103*, 203−216.
Negele, J. C., Dotson, D. G., Liu, W., Sweeny, H. L., & Putkey, J. A. (1992) *J. Biol. Chem. 267*, 825−831.
Neri, D., Szyperski, T., Ottig, G., Senn, H., & Wuthrich, K. (1989) *Biochemistry 28*, 7510−7516.
Nicholls, A. (1992) *GRASP: graphical representation and analysis of surface properties*, Columbia University, New York.
Nilges, M., Gronenborn, A. M., Brünger, A. T., & Clore, G. M. (1988) *Protein Eng. 2*, 27−38.

Pascal, S. M., Muhandiram, D. R., Yamazaki, T., Forman-Kay, J. D., & Kay, L. E. (1994) *J. Magn. Reson., Ser. B 103*, 197−201.
Pollesello, P., Ovaska, M., Kaivola, J., Tilgmann, C., Lundstrom, K., Kalkkinen, N., Ulmanen, I., Nissinen, E., & Taskinen, J. (1994) *J. Biol. Chem. 269*, 28584−28590.
Potter, J. D., & Gergely, J. (1975) *J. Biol. Chem. 250*, 4628−4633.
Putkey, J. A., Sweeny, H. L., & Campbell, S. T. (1989) *J. Biol. Chem. 264*, 12370−12378.
Putkey, J. A., Liu, W., & Sweeny, H. L. (1991) *J. Biol. Chem. 266*, 14881−14884.
Rao, V. G., Akella, A. B., Su, H., & Gulati, J. (1995) *Biochemistry 34*, 562−568.
Satyshur, K. A., Rao, S. T., Pyzalska, D., Drendal, W., Greaser, M., & Sundralingham, M. (1988) *J. Biol. Chem. 263*, 1628−1647.
Shaka, A. J., Keeler, J., Frenkiel, T., & Freeman, R. (1983) *J. Magn. Reson. 52*, 335−338.
Shrake, A., & Rupley, J. A. (1973) *J. Mol. Biol. 79*, 351−371.
Sia, S. K., Li, M. X., Spyracopoulos, L., Gagné, S. M., Liu, W., Putkey, J. A., & Sykes, B. D. (1997) *J. Biol. Chem. 272*, 18216−18221.
Skelton, N. J., Kördel, J., Akke, M., Forsén, S., & Chazin, W. J. (1995) *Nat. Struct. Biol. 1*, 239−245.
Slupsky, C. M., & Sykes, B. D. (1995) *Biochemistry 34*, 15953−15964.
Slupsky, C. M., Kay, C. M., Reinach, F. C., Smillie, L. B., & Sykes, B. D. (1995a) *Biochemistry 34*, 7365−7375.
Slupsky, C. M., Reinach, F. C., Smillie, L. B., & Sykes, B. D. (1995b) *Protein Sci. 4*, 1279−1290.
Strynadka, N. C. J., Chernaia, M., Sielecki, A. R., Li, M. X., Smillie, L. B., & James, M. N. G. (1997) *J. Mol. Biol.* (in press).
Szczensna, D., Guzman, G., Millet, T., Zhao, J., Farokhi, K., Ellemberger, H., & Potter, J. D. (1996) *J. Biol. Chem. 271*, 8381−8386.
Tobacman, L. S. (1996) *Annu. Rev. Physiol. 58*, 447−481.
van Eerd, J.-P., & Takahashi, K. (1975) *Biochem. Biophys. Res. Commun. 64*, 122−127.
Vuister, G. W., & Bax, A. (1993) *J. Am. Chem. Soc. 115*, 7772−7777.
Wittekind, M., & Mueller, L. (1993) *J. Magn. Reson., Ser. B 101*, 201−205.
Zhang, M., Tanaka, T., & Ikura, M. (1995) *Nat. Struct. Biol. 2*, 758−767.
Zhang, O., Kay, L. E., Olivier, J. P., & Forman-Kay, J. D. (1994) *J. Biomol. NMR 4*, 845−858.
Zot, A. S., & Potter, J. D. (1987) *Annu. Rev. Biophys. Biophys. Chem. 16*, 535−559.

BI971223D